

iltonian for an ideal YIG sphere magnetized along the [100] axis is symmetric relative to rotation about this axis. A symmetric distribution of PSW's is described in Ref. 1. The PSW distribution found above does not have this symmetry. The asymmetry indicates either that there is a spontaneous violation of the symmetry in the PSW system or that the crystals are characterized by a weak anisotropy which appears during their "firing" and is due to the imperfect treatment of the samples; this anisotropy is sufficient to disturb the symmetry of the distribution. The S approximation (see Ref. 1) is used in Ref. 4 to show that a symmetric PSW distribution in crystals with the same symmetry as ours is unstable, but singular distributions in the form of a finite number of pairs of spin waves with mutually perpendicular spin vectors may be stable. This means that the PSW system does indeed experience spontaneous symmetry breaking. The consequence may be an anisotropy of the attenuation coefficient of spin waves (associated with the hard excitation of PSW's) ensuring an additional stability of the asymmetric PSW distribution. The crystal anisotropy which disturbs the Hamiltonian symmetry enhances the influence of the spontaneous symmetry breaking. Separation of the contribution of these two mechanisms is not possible on the basis of the available experimental data.

The experiments indicate that there is no doubled-frequency radiation in a magnetic field whose intensity corresponds to the coalescence of two spin waves with angles φ_k differing by about $\pi/2$. The emission of such radiation would have indicated the presence of two pairs of PSW packets corresponding to the asymmetric solutions in the form of a quartet of waves, as found in Ref. 4. It is possible that the intensity of this radiation is

far too low to be recorded reliably or that only one pair of waves is excited in our experiments.

Scattering of spin waves by inhomogeneities in a crystal and by thermal spin waves can explain why the PSW distribution in respect of φ_k and θ_k is not singular and why the broadening $\Delta\varphi_k$ and $\Delta\theta_k$ is finite, depending strongly on the pumping rate and quality of the crystal. The distribution function of thermal spin waves is closely related to the PSW distribution and may vary considerably with the pumping rate. The probability of scattering of spin waves by inhomogeneities, considered in Ref. 5, may be associated with the line width ΔH_{ks} . The formulas of Ref. 5 and the experimental values of $\Delta\theta_k$ allow us to estimate ΔH_{ks} . For our crystals, we find that $\Delta H_{ks} \leq 10^{-2} \Delta H_k$.

A theory explaining the finite value of $\Delta\varphi_k$ and relating it to some physical characteristics of a crystal should help in developing a new very sensitive method for quality control of ferrite single crystals.

- ¹V. E. Zakharov, V. S. L'vov, and S. S. Starobinets, *Usp. Fiz. Nauk* **114**, 609 (1974) [*Sov. Phys. Usp.* **17**, 896 (1975)].
²G. A. Melkov and V. L. Grankin, *Zh. Eksp. Teor. Fiz.* **69**, 1415 (1975) [*Sov. Phys. JETP* **42**, 721 (1975)].
³E. Schlömann and R. I. Joseph, *J. Appl. Phys.* **32**, 1006 (1961).
⁴A. S. Bakal', *Zh. Eksp. Teor. Fiz.* **74**, 993 (1978) [*Sov. Phys. JETP* **47**, 522 (1978)].
⁵V. E. Zakharov and V. S. L'vov, *Fiz. Tverd. Tela (Leningrad)* **14**, 2913 (1972) [*Sov. Phys. Solid State* **14**, 2513 (1973)].

Translated by A. Tybulewicz

Character of submillimeter photoconductivity in *n*-InSb

E. M. Gershenzon, V. A. Il'in, L. B. Litvak-Gorskaya, and S. R. Filonovich

Moscow State Pedagogical Institute

(Submitted 6 July 1978)

Zh. Eksp. Teor. Fiz. **76**, 238-250 (January 1979)

A comprehensive investigation was made of the submillimeter photoconductivity of *n*-InSb in the range of wavelengths $\lambda = 0.6-8$ mm, magnetic fields $H = 0-30$ kOe, electric fields $E = 0.01-0.5$ V/cm, and temperatures $T = 1.3-30$ K. The kinetics of the photoconductivity processes as a function of T , E , and H is investigated. It is shown that impurity photoconductivity does exist for any degree of compensation of extremely purified *n*-InSb. Particular attention is paid to the hopping photoconductivity realized in strongly compensated *n*-InSb ($K > 0.8$).

PACS numbers: 72.40.+w, 72.80.Ey

1. INTRODUCTION

Indium antimonide of *n*-type (*n*-InSb) occupies at present a special position among the semiconductors. In its electrophysical properties, it is a unique object for investigations and applications, because it combines isotropy of the conduction band with small effective mass of the free electrons, $m = 0.013 m_0$, and its crystal lat-

tice has an appreciable permittivity, $\kappa = 16$, and consequently a large Bohr radius $a = 640 \text{ \AA}$ of the electron at the hydrogenlike impurity centers. The concentration N_d of the residual donors in extremely purified *n*-InSb is $\sim 10^{14} \text{ cm}^{-3}$, and their compensation is $K = N_a/N_d = 0.3-0.7$. A relatively small change of N_d and K , and also of the external conditions (temperature T , magnetic field H , electric field E , etc.) leads to substantial

changes in the conductivity of the material, something unattainable in other semiconductors. Consequently n -InSb is used in many devices, including a photoreceiver, cooled to helium temperatures, of electromagnetic radiation in the millimeter and submillimeter bands.

Submillimeter photoconductivity (PC) in n -InSb was observed by Putley in 1960.¹ The observed PC differed from that previously investigated in Ge and Si. The photoconductivity in n -InSb exists at a quantum energy $\hbar\omega \sim \varepsilon_d$ ($\varepsilon_d = 1 \text{ Ry} = 0.67 \text{ MeV}$ is the ionization energy of an isolated donor), but there is no "red boundary" of the photoeffect. The photoconductivity remains practically unchanged in the electromagnetic wavelength range $\lambda = 0.5\text{--}8.0 \text{ mm}$ ($\hbar\omega = \varepsilon_d$ corresponds to $\lambda = 2 \text{ mm}$). The unusual character of the photoconductivity gave rise to extensive discussions concerning the detection mechanism.²⁻¹³ The viewpoint established as a result was that the photoconductivity is produced in n -InSb by a "heating" mechanism. Its gist is the following: the impurity states in n -InSb with donor density $N_d \approx (1\text{--}2) \times 10^{14} \text{ cm}^{-3}$ form a single continuum with the conduction band, so that at $T \approx 4.2 \text{ K}$ the conductivity is produced by the free electrons, whose concentration $n = N_d - N_a$ remains unchanged. The radiation changes the mobility μ of the electrons, and gives rise to " μ photoconductivity"; the idea of the existence of μ photoconductivity in n -InSb was first advanced by Rollin,² and the detailed theory was developed by Kogan.³

Although the theory of μ photoconductivity has explained some features of the photoconductivity in n -InSb, a number of the experimental results could not be fitted within its framework. In particular, it did not lead to an increase of the photoconductivity signal with increasing compensation^{6,9} and with decreasing temperature,^{9,12} nor did it lead to the observed frequency dependence of the absorption coefficient $\alpha(\lambda)$.⁷ Nonetheless the advent of the theory of μ photoconductivity is no accident. In fact, the purest n -InSb should have in the absence of compensation metallic conductivity ($N_d \approx 0.03\text{--}0.04$).¹⁴ The material, however, is always compensated, with $K = 0.3\text{--}0.99$. The role of this compensation was understood only following the work of Anderson,¹⁵ Mott,¹⁴ and Éfros and Shklovskii,^{16,17} who have shown that the large fluctuation potential due to the compensation should lead to localization of impurity states and to a loss of the metallic conductivity.

Subsequent measurements have shown that the impurity states in n -InSb that is purified and compensated to the limit are localized,¹⁸ and that the conductivity at helium temperatures is of the impurity type. Its form is determined by the compensation. On the basis of galvanomagnetic and spectral investigations¹⁸⁻²¹ it was proved that static conductivity is realized by three basic mechanisms.

(1) At $K < 0.8$ and sufficiently low T , the conductivity is via conducting impurity band (the so-called ε_2 band) and the ground states of the electrons on the donors are localized and form the ε_3 band.¹⁹

(2) At $0.8 \lesssim K \lesssim 0.95$, in a definite temperature region,

hopping conductivity over the impurity percolation level takes place, is characterized by an activation energy ε_3 , and goes over with further decrease of T into a hopping conductivity with an activation energy that decreases as $T \rightarrow 0$ (Mott conductivity²²).

(3) At $K > 0.99$ and $T \lesssim 20 \text{ K}$, Mott hopping conductivity is realized. This impurity-conductivity mechanism is realized also in strongly doped and compensated n -InSb.

Two new models were proposed recently, for photoconductivity in n -InSb. An intraband photoconductivity was considered in Refs. 10-12 but is applicable only to strongly doped and strongly compensated material ($Na^3 \gg 1$). According to this model, the electrons are evaporated by the radiation from electron drops that are insulated from one another, become free, and participate in the photoconductivity. The attempts made in Ref. 12, to apply this theory to extremely purified n -InSb, are in our opinion untenable.

In our earlier paper¹³ we advanced the hypothesis that hopping photoconductivity¹⁹ wherein the photocarriers as well as the equilibrium carriers move over localized impurity states is realized in compensated n -InSb. The hopping-photoconductivity model explains the main features of the photoconductivity in n -InSb, namely the absence of the red boundary, the dependence on the compensation, etc.

The present paper is a continuation and a development of Ref. 13. We investigated the photoconductivity in n -InSb purified to the limit, at any degree of compensation, and studied the spectra of the photoconductivity, its kinetics, etc.

We note that at the present time there is practically no theory of hopping photoconductivity. Comprehensive investigations of the photoconductivity are therefore needed in a wide range of wavelengths, of electric and magnetic field intensities, and of temperatures. A comparison of the features of photoconductivity with the character of static conductivity is also needed.

2. MEASUREMENT PROCEDURE AND SAMPLES

We investigated the dependence of the photoconductivity signal ΔU_{ph} (U is the bias on the sample) on the magnetic field H ($H = 0\text{--}20 \text{ kOe}$), on the temperature T ($T = 1.3\text{--}30 \text{ K}$), and on the radiation wavelength λ ($\lambda = 0.6\text{--}8 \text{ mm}$). We investigated also the dependence of the absorption coefficient α on H and T and of the photoconductivity relaxation time τ_{ph} on H , T , E , and λ . For the spectrum measurements we used spectrometers with backward-wave tubes²⁵ and with klystrons.²⁰ The samples were shielded against the short-wave radiation.

1. To measure the $\Delta U_{ph}(\lambda)$ dependence we used a procedure in which the same sample was used to equalize the power level with changing λ and to measure $\Delta U_{ph}(\lambda)$. The choice of this procedure was dictated by the presence of interference effects in the quasioptical channels. The procedure is based on the fact that when a sample with $K < 0.95$ is subjected to an electric field exceeding a certain critical value E_{br} , impurity breakdown takes place.²⁶ In this regime, it is possible to ob-

tain the photoresponse $\Delta U_{ph}(E > E_{br})$ due to the absorption of the radiation by the free electrons. The spectrum of this signal is determined completely by the dependence of the coefficient $\alpha_{free}(\lambda)$ of absorption of the radiation by the free electrons. It is known²⁷ that in the considered wavelength region $\alpha_{free}(\lambda)$ decreases monotonically with decreasing λ . The experimental $\alpha_{free}(\lambda)$ dependence can be determined by the procedure described in Ref. 20.

The procedure for the measurement of $\Delta U_{ph}(\lambda)$ is the following. The field at the n -InSb sample is raised to $E > E_{br}$. An attenuator in the spectrometer channel regulates the power incident on the sample and sets a certain signal level $\Delta U_{ph}(E > E_{br})$ which is maintained constant while λ is varied. The value of E is then decreased until the sample resistance is independent of the bias, and ΔU_{ph} is measured. These operations are carried out for each wavelength. Knowing the $\alpha_{free}(\lambda)$ dependence, corrections can be introduced for the monotonic increase of the power when the signal $\Delta U_{ph}(E > E_{br})$ is maintained constant with decreasing λ . This procedure yields quite reliable information on the presence of any nonmonotonicity in the $\Delta U_{ph}(\lambda)$ spectra, although it does not make it possible to determine with high accuracy the ratio of the peak intensities.

2. $\Delta U_{ph}(H)$ was measured by a standard modulation procedure (the frequency of the radiation modulation was 400–450 Hz), with continuous scanning the magnetic field of the superconducting solenoid ($H \approx 30$ kOe). The signal was recorded with an electronic potentiometer. The function $\alpha(H)$ was determined from a comparison of the signals from two identical samples placed one behind the other.²⁰ The measurements of $\Delta U_{ph}(H)$ and $\alpha(H)$ were carried out in a current-generator regime for the ac component and a voltage-generator regime for the dc component.²⁸

3. The photoconductivity relaxation time τ_{ph} was determined from the dependence of the signal ΔU_{ph} on the radiation-modulation frequency by the procedure described in Ref. 29.

The n -InSb samples were cut in the form of plates measuring $7.2 \times 3.4 \times 1$ mm, ground, and etched in CP-4A. The sample parameters are listed in the table. The donor concentration N_d in samples 1–3 was determined from the temperature dependence of the mobility in the region $T = 1.5$ –30 K (Ref. 30); in samples 4–8 it was determined from the distribution curve of the donors along the InSb ingot.³¹

As seen from the table, we investigated in the present study n -InSb of extremely high purity, with $N_d \approx 7 \cdot 10^{13}$

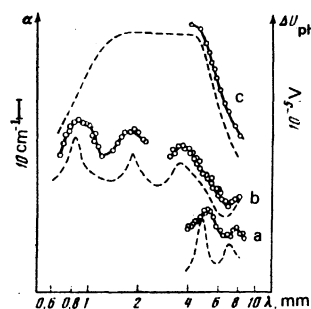


FIG. 1. Spectral dependences of the photoresponse $\Delta U_{ph}(\lambda)$ (solid curves) and of the absorption coefficient $\alpha(\lambda)$ (dashed) at $T = 1.5$ K: a) sample I-1, b) II-4, c) III-6.

$-2 \cdot 10^{14} \text{ cm}^{-3}$; groups I–III are characterized by different mechanisms of static conductivity, as noted in the Introduction.

3. EXPERIMENTAL RESULTS

To determine the mechanism of the photoconductivity in n -InSb we must identify the starting states for the photoexcited electrons and the states over which the photoconductivity is realized.

1. The answer to the first question can be obtained by comparing the spectral dependences of the photoconductivity signal and the absorption signal $\alpha(\lambda)$.

Figure 1 shows plots of $\Delta U_{ph}(\lambda)$ and $\alpha(\lambda)$ at $T = 1.5$ K for samples I-1, II-4, and III-6. It is seen that $\Delta U_{ph}(\lambda)$ and $\alpha(\lambda)$ curves for each sample are similar, but the photoconductivity peaks are much broader than the corresponding absorption peaks.

A comparison of the position of the absorption peak and the photoconductivity peak for sample I-1 (curves a) with the characteristic static-conductivity activation energy (see the table) allows us to conclude that the short-wave peak ($\lambda = 5$ mm) is due to photoionization of the impurity centers, while the long-wave peak ($\lambda = 7$ mm) is due to the transition of the electrons from the ϵ_2 band into the conduction band. Thus, in the samples of this group, the starting states are either those of the conducting (ϵ_2) impurity band or of the impurity band of the ground states of the impurities (ϵ_3 band¹⁴).

For more strongly compensated samples (group II), the behavior of $\Delta U_{ph}(\lambda)$ and $\alpha(\lambda)$ is illustrated with sample II-4 as the example (curves b). As shown in Ref. 21, in such samples the absorption at sufficiently low temperatures is determined by the donor pairs of the type of the molecular-hydrogen ion H_2^+ . The $\alpha(\lambda)$ peak at $\lambda \approx 0.85$ mm corresponds to photoionization of H_2^+ centers with a characteristic distance $R_{av} \approx 2a$ between "nuclei." The longer-wavelength absorption peaks are connected with transitions from the ground ($1s\sigma_g$) state to the excited states of the H_2^+ center. A feature of the photoconductivity curves is the existence of a photoconductivity signal at radiation-quantum energies much lower than the ionization energy. At the same time, the agreement between the positions of the $\Delta U_{ph}(\lambda)$ and $\alpha(\lambda)$ peaks is evidence that the starting states for the photoconductivity are $1S\sigma_g$, and even intramolecular transitions give rise to photoconductivity.

TABLE I.

Sample no.	$(N_d - N_a) \times 10^{-14}, \text{ cm}^{-3}$	$\mu_{77} K \cdot 10^{-1}, \text{ cm}^2/V \cdot \text{sec}$	$N_d \cdot 10^{-14}, \text{ cm}^{-3}$	$K = \frac{N_a}{N_d}$	Activation energy, meV		
					ϵ_1	ϵ_2	ϵ_3
I-1	9	6.8	2	0.6	0.25	0.06	—
I-2	3.4	11.5	0.7	0.23	0.4	0.05	—
II-3	2.2	4.5	1.5	0.85	1.4	—	0.5
II-4	1.3	4.2	1.2	0.89	2.0	—	1.0
II-5	1.3	4.0	1.5	0.9	2.0	—	1.1
III-6	~ 0.1	3.5	1.4	0.96	4	—	—
III-7	< 0.1	2.9	1.5	~ 0.99	20	—	—
III-8	$\sim 10^{-2}$	2.7	1.4	> 0.99	20	—	—

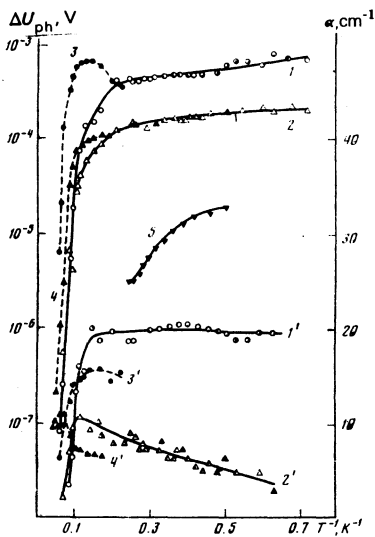


FIG. 2. Temperature dependence of the photoresponse ΔU_{ph} (unprimed numbers of curves) and of the absorption coefficient α (primed numbers): 1) sample II-3, $\lambda=1$ mm; 2) II-3, 8 mm; 3) III-7, 1 mm; 4) III-7, 8 mm; 5) I-2, 8 mm.

The plots of $\Delta U_{ph}(\lambda)$ and $\alpha(\lambda)$ for sample III-6 (curves c) differ substantially from those considered above. The bell shape of the $\alpha(\lambda)$ is typical of the absorption of radiation of electrons localized near the Fermi level ϵ_F .^{32,33} The similarity of the $\Delta U_{ph}(\lambda)$ and $\alpha(\lambda)$ curves shows that the photoconductivity of the samples of this group is connected with the same starting states.

Thus, an analysis of the frequency dependences shows that the photoconductivity starting states for all the sample groups are impurity states.²⁾

2. The identification of the states over which the photoconductivity is realized is a more complicated problem. The determination of these states has called for a comprehensive investigation of the dependences of the photoconductivity on the external conditions.

Figure 2 shows plots of $\Delta U_{ph}(T)$ and $\alpha(T)$ for samples II-3 and III-7 at $\lambda=1$ and 8 mm. It is seen that for sample II-3 the character of $\Delta U_{ph}(T)$ does not depend on λ : the weak decrease of the photoconductivity signal when the temperature is increased to $T \sim 5$ K gives way to an abrupt decrease at $T \geq 10$ K (ΔU_{ph} decreases by a factor of more than 100 in the interval 10–20 K). The $\alpha(T)$ plots of sample II-3 for the same wavelengths are different. Whereas at $\lambda=1$ mm and $T \leq 7$ K the value of α is practically constant, at $\lambda=8$ mm and $T \approx 10$ K the $\alpha(T)$ curve has a maximum. At $T > 10$ K, the value of α decreases sharply with increasing T , in analogy with ΔU_{ph} .

The plots of $\Delta U_{ph}(T)$ and $\alpha(T)$ for sample III-7 at $\lambda=8$ mm are similar to the corresponding curves of sample II-4, but the maximum on $\alpha(T)$ and the start of the abrupt decrease of ΔU_{ph} as a function T occur at higher values of T . At $\lambda=1$ mm $\Delta U_{ph}(T)$ and $\alpha(T)$ are characterized by a maximum at $T=8$ K. The difference between the $\alpha(T)$ curves at different λ , in our opinion, correlates with the change of the position of the bell-shaped $\alpha(\lambda)$ with changing temperature (see Fig. 1 and Ref. 21).

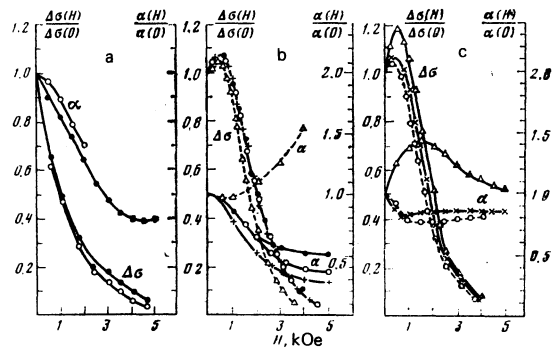


FIG. 3. Plots of $\Delta\sigma(H)/\Delta\sigma(0)$ and $\alpha(H)/\alpha(0)$ at $T=1.7$ K: a) sample I-2, \circ — $\lambda=0.6$ mm, \bullet — $\lambda=1.0$ mm; b) sample II-3, \circ — $\lambda=0.87$ mm, $+$ — $\lambda=1.1$ mm, \bullet — $\lambda=1.8$ mm, Δ — $\lambda=8$ mm; c) sample III-7, Δ — $\lambda=0.6$ mm, \times — $\lambda=1.2$ mm, \circ — $\lambda=2.3$ mm.

Figure 2 shows also a plot of $\Delta U_{ph}(T)$ of sample I-2 at $\lambda=8$ mm. It is seen that ΔU_{ph} decreases with increasing T , and no region of weak temperature dependence is observed.

Important data helping to explain the photoconductivity mechanism are provided by measurements of $\Delta U_{ph}(H)$ and $\alpha(H)$. Figure 3 shows, for several values of λ , plots³⁰ of $\Delta\sigma(H)=\sigma(H)\Delta U_{ph}(H)/U$ and $\alpha(H)$ of samples I-2, III-3, and III-7 at $T=1.7$ K and $H=0-5$ kOe. It is seen that for all the samples the value of $\Delta\sigma(H)$ decreases substantially with increasing H and it is approximately the same for all λ . The $\Delta\sigma(H)/\Delta\sigma(0)$ curves of sample II-2 coincide at $\lambda \leq 2$ mm. In weak fields H , the samples of groups II and III show increases⁴⁾ of $\Delta\sigma$ with increasing H .

The $\alpha(H)$ dependences are not the same for the considered sample groups. For the first two groups at $\lambda < 2$ mm the value of $\alpha(H)$ decreases with increasing H , while for the samples of the third group, as well as of the second at $\lambda=8$ mm, $\alpha(H)$ is practically constant or else increases with H . The relative changes of α with changing H are small compared with the changes of $\Delta\sigma$.

A study of the dependence of the photoconductivity relaxation time τ_{ph} on the external conditions (T, E, H) yields additional information on the photoconductivity mechanisms.

Figure 4 shows plots of $\tau_{ph}(E)$ for samples from different groups. In sample I-2 at small E , the value of

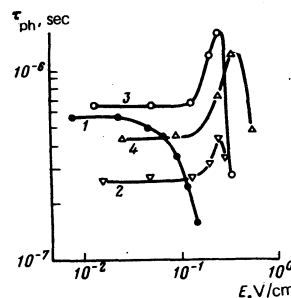


FIG. 4. Dependence of the photoconductivity relaxation time τ_{ph} on the electric field ($T=4.2$ K): 1—sample I-2, $\lambda=8$ mm; 2—sample II-3, $\lambda=1$ mm; 3—sample II-3, $\lambda=8$ mm; 4—sample III-7, $\lambda=8$ mm.

τ_{ph} does not depend on E ; when impurity breakdown sets in, an abrupt decrease of τ_{ph} is observed (curve 1). The plots of τ_{ph} for samples II-3 and III-7 (curves 2-4) have different growth rates of $\tau_{ph}(E)$ in the field region preceding the impurity breakdown. The values of τ_{ph} for samples with different K differ insignificantly at small values of E : the range of τ_{ph} is $(3-7) \times 10^{-7}$ sec. The presented measured values of τ_{ph} are not connected with effects on the surface: the values of τ_{ph} are the same for samples with thickness 1-0.1 mm.

The temperature dependence of τ_{ph} was investigated for samples of groups II and III. For samples of group II at $\lambda \leq 8$ mm, a maximum of τ_{ph} is observed at $T \approx 7$ K. At $\lambda = 8$ mm the values of τ_{ph} of these samples, just as those of group III at arbitrary λ , are practically constant to $T \leq 7-10$ K, beyond which they decrease sharply. The start of the decrease of τ_{ph} in the samples of group III corresponds to higher T .

The investigations have shown that in the samples of groups II and III the value of τ_{ph} in weak magnetic fields (up to $H \sim 4$ kOe) are practically constant.

The presented experimental results of the comprehensive investigation of samples with greatly differing compensations (groups I-III) cannot be attributed only to the motion of the photoelectrons in the conduction band. At the same time, the existence of photoconductivity at quantum energies $\hbar\omega \ll \epsilon_F$ is evidence that it is determined by the motion of the photoelectrons over the impurity states. However, the difference between the plots of $\Delta U_{ph}(T, H)$, $\alpha(T, H)$, and $\tau_{ph}(E)$ for samples of different groups and of $\Delta U_{ph}(\lambda)$ and $\alpha(\lambda)$ within each group show that there exist several mechanisms of photoconductivity over the impurity states. It will be shown below that in strongly compensated n -InSb the photoconductivity can be explained within the framework of the model of hopping photoconductivity¹³; in weakly compensated n -InSb, the photoconductivity is due to the motion of the photoexcited electrons in the conducting impurity band.

4. HOPPING PHOTOCONDUCTIVITY MODEL

In this section an attempt is made to estimate the photoconductivity for the simplest situations, when the radiation-induced conductivity mechanism does not differ from the static-conductivity mechanism, and to ascertain the influence of external factors on the hopping photoconductivity.

We regard hopping photoconductivity as a process similar to static hopping conductivity, the only difference being that a photon must be absorbed in order for the electron to go over into a higher energy state. Under equilibrium conditions it is possible to introduce for the hopping of the electron over the impurity centers the diffusion coefficient¹⁴

$$D \approx \frac{1}{6} \nu_{\text{phon}} R^2 \exp\left[-\frac{2R}{a^*} - \frac{\Delta W}{kT}\right], \quad (1)$$

where ν_{phon} is a factor that depends on the phonon spectrum, R is the average length of the electron hop, ΔW is the difference between the energies of the final and

initial states, and a^* is the characteristic falloff length of the wave functions of the states over which the hopping photoconductivity takes place.

Using the Einstein relation $\mu = eD/kT$, we can write an expression for the mobility of the electrons hopping over the localized states:

$$\mu_n = \frac{1}{6} \nu_{\text{phon}} \left(\frac{eR^2}{kT}\right) \exp\left[-\frac{2R}{a^*} - \frac{\Delta W}{kT}\right]. \quad (2)$$

To calculate σ we must estimate the concentration of the electrons that take part in the conductivity. Mott and Davis¹⁴ propose that this concentration is equal to $N(\epsilon_F)kT$ [$N(\epsilon_F) \approx \text{const}$ is the density of states near the Fermi level]. Then

$$\sigma = \frac{1}{6} \nu_{\text{phon}} \left(\frac{e^2 R^2}{kT}\right) \exp\left[-\frac{2R}{a^*} - \frac{\Delta W}{kT}\right] N(\epsilon_F) kT. \quad (3)$$

Expression (3) can be made more detailed for a concrete form of the hopping conductivity.

In the case of ϵ_3 conductivity, the electron goes over to the nearest impurity center, therefore $R \sim (N_d)^{-1/2}$, and $N(\epsilon_F) \approx (N_d - N_a)/\epsilon_3$.¹⁷

In the case of Mott hopping conductivity, the average length R of the electron hop is determined by the relation

$$^{1/3} \pi R^3 N(\epsilon_F) \Delta W = 1,$$

and in this case $R \approx a(T_0/T)^{1/4}$, where $kT_0 = 16/N(\epsilon_F)a^3$.

The concentration of the nonequilibrium electrons in hopping photoconductivity can be defined as

$$\Delta n = \alpha q \beta \tau_{ph}, \quad (4)$$

where q is the photon flux per unit sample surface, β is the quantum yield, which we assume equal to unity, and τ_{ph} is the photoconductivity relaxation time.

The photoelectron mobility depends in practice only on the degree of overlap of the wave functions of the initial and final states:

$$\mu_{ph} \sim \frac{eR^2}{kT} \nu_{\text{phon}} \exp\left[-\frac{2R}{a^*}\right]. \quad (5)$$

It is assumed here that in the case of photoconductivity through an impurity percolation level the hop is to the nearest center, just as in the case of static conductivity in the dark (ϵ_3). In the case of photoconductivity over the states near the Fermi level, the average length of the hop, generally speaking, differs from the equilibrium value. At $T=0$ we have according to Ref. 32

$$R \approx [^{1/3} \pi N(\epsilon_F) \hbar\omega]^{-1/2}. \quad (6)$$

If $T > 0$, then R increases somewhat because some of the states are occupied. A numerical calculation shows that in the interval $2 \leq T \leq 10$ K the length is $R \approx 1.4R_{T=0}$ and hardly changes with T .

Using relations (3)-(6) we can obtain expressions for the relative photoresponse in hopping photoconductivity (in the current-generator regime). In the case of photoconductivity through the percolation level we have

$$\frac{\Delta U_{ph}}{U} = \frac{\alpha q \tau_{ph} \epsilon_3}{N_d - N_a} \exp\left(\frac{\epsilon_3}{kT}\right); \quad (7)$$

in the case of photoconductivity over the states near the Fermi level⁵ we have

$$\frac{\Delta U_{ph}}{U} \approx 4 \cdot 10^{-2} \frac{\alpha q \tau_{ph} a^{*2} (kT_0)^{3/2}}{(\hbar\omega)^{3/2} (kT)^{1/2}} \times \frac{\exp[(T_0/T)^{3/2}]}{\exp[1/2 (kT_0/\hbar\omega)^{1/2}]} \quad (8)$$

It is clear that hopping photoconductivity can exist at any quantum energy. It is useful to characterize the magnitude of the hopping conductivity by the ratio of the photoresponse to the incident power P ($\Delta U_{ph}/P = S_u$, the volt-watt sensitivity). Using the parameters given in the table for the samples of groups II and III and using the experimentally determined values of α and τ_{ph} , we can calculate S_u in the frequency range of interest to us for the cases considered here. An estimate for $T \sim 4$ K yields $S_u \geq 10^8$ V/W.

It should be noted that estimates yield a rather high sensitivity of the sample to radiation under conditions in which the hopping photoconductivity is of the same type as the static conductivity. On the other hand, if the mechanism of conductivity induced by the radiation differs from the mechanism of static conductivity, then the sensitivity can be higher.

5. DISCUSSION OF EXPERIMENTAL RESULTS

The presented experimental results and estimates enable us to analyze a group of phenomena that characterize photoconductivity in n -InSb, and to ascertain through which states the photoconductivity is realized. For this purpose it is necessary to consider above all the dependences of the photocarrier mobility μ_{ph} on T and H .

The first of them, $\mu_{ph}(T)$, can be determined in the case of the photoionization mechanism by measuring simultaneously $\Delta U_{ph}(T)$, $\sigma(T)$, $\alpha(T)$ and $\tau_{ph}(T)$:

$$\frac{\mu_{ph}(T)}{\mu_{ph}(T_1)} = \frac{\Delta U_{ph}(T)}{\Delta U_{ph}(T_1)} \frac{\sigma(T)}{\sigma(T_1)} \frac{\alpha(T_1)}{\alpha(T)} \frac{\tau_{ph}(T_1)}{\tau_{ph}(T)}$$

where $T_1 = 4.2$ K.⁶⁾

Figure 5 shows the corresponding curves for samples II-3 ($\lambda = 1$ and 8 mm) and III-7 ($\lambda = 8$ mm), obtained using the data of Fig. 2 and measurements of the $\tau_{ph}(T)$ dependence.

The relative change of the mobility of the photocarriers in the magnetic field

$$\frac{\mu_{ph}(H)}{\mu_{ph}(0)} = \frac{\Delta U_{ph}(H)}{\Delta U_{ph}(0)} \frac{\sigma(H)}{\sigma(0)} \frac{\alpha(0)}{\alpha(H)} \frac{\tau_{ph}(0)}{\tau_{ph}(H)}$$

can be obtained from measurements of $\Delta U_{ph}(H)$, $\sigma(H)$,

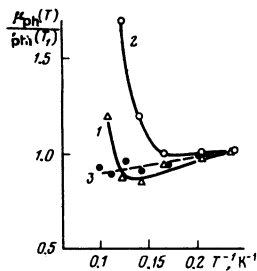


FIG. 5. Plot of $\mu_{ph}(T)/\mu_{ph}(T_1)$ ($T_1 = 4.2$ K): 1—sample II-3, $\lambda = 1$ mm; 2—sample II-3, $\lambda = 8$ mm; 3—sample III-7, $\lambda = 8$ mm.

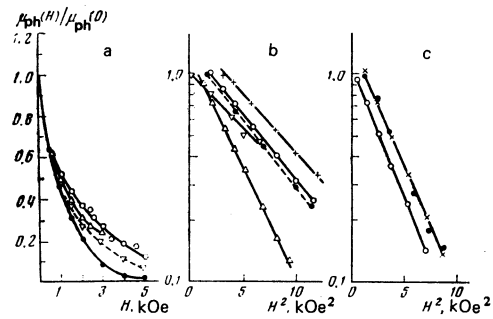


FIG. 6. Plot of $\mu_{ph}(H)/\mu_{ph}(0)$ ($T = 1.7$ K): a) sample I-2: ●— $\lambda = 1$ mm, ○— $\lambda = 3$ mm, △— $\lambda = 8$ mm, ▽— $\sigma(H)/\sigma(0)$; b) sample II-3: ○— $\lambda = 0.87$ mm, +— $\lambda = 1.1$ mm, ●— $\lambda = 1.8$ mm; △— $\lambda = 8$ mm, ▽— $\sigma(H)/\sigma(0)$; c) sample III-7: ○— $\lambda = 0.6$ mm, ×— $\lambda = 1.24$ mm, ●— $\lambda = 2.3$ mm.

$\alpha(H)$, and $\tau_{ph}(H)$; the corresponding plots are shown in Fig. 6 for samples I-2, II-3, and III-7 at several values of λ (we used the data of Fig. 3 and the independence of τ_{ph} of H , mentioned in Sec. 3). The shapes of the plots pertaining to samples of groups II and III is typical of hopping conductivity: μ_{ph} is practically independent of T (at $T \leq 8-10$ K) [see (5)], and $\ln \mu_{ph} \sim H^2$ (Ref. 17).

In addition, the independence of μ_{ph} of T precludes a contribution of photothermal ionization of the impurities³⁵ to the photoconductivity at $T \leq 8-10$ K. The shapes of the $\mu_{ph}(H)$ curves for samples from different groups are different: whereas for sample II-3 at quantum energies $\hbar\omega \geq 0.6$ MeV ($\lambda \leq 2$ mm) the slopes of all the $\mu_{ph}(H)/\mu_{ph}(0)$ curves are equal, at $\hbar\omega = 0.16$ MeV ($\lambda = 8$ mm) they differ substantially. For the more compensated samples (group III) and for the weakly compensated samples (group I), whose $\mu_{ph}(H)$ dependence is not exponential, the shape of the curves depends little on the values of the radiation quanta, even at the smallest values of $\hbar\omega$.

The similarity of the shape of the $\mu_{ph}(H)$ curves pertaining different λ for sample I-2, and the equality of their slopes for samples II-3 and III-7, indicate that in each group of samples the photoconductivity is effected through the same states, regardless of the energy of the exciting quantum.

In the case of static hopping conductivity it is known¹⁷ that for conductivity through the percolation level we have

$$\frac{\sigma(H)}{\sigma(0)} = \frac{\mu_h(H)}{\mu_h(0)} = \exp\left[-\frac{t_1 a e^2 H^2}{N_a c^2 \hbar^2}\right], \quad t_1 = \text{const.} \quad (9)$$

For conductivity through states near the Fermi level

$$\frac{\mu_h(H)}{\mu_h(0)} = \exp\left[-2 \cdot 10^{-3} \frac{e^2 a^* H^2}{c^2 \hbar^2} \left(\frac{T_0}{T}\right)^{3/2}\right]. \quad (10)$$

If the photoconductivity mechanism is the same as that of the static conductivity, then relations (9) and (10) are valid also for photoelectrons. From the slopes of the $\mu_{ph}(H)/\mu_{ph}(0)$ curves we can then determine the length of falloff of the wave functions of the states a_{ph} and a_{ph}^* , which ensures photoconductivity hops at different photoconductivity mechanisms, and compare them with the corresponding values of a and a^* which are typical of static conductivity.

For sample II-3 at $\lambda < 2$ mm ($\hbar\omega > \varepsilon_3$) we have $a_{ph} = 680$ Å. Analysis of the dependence of the ε_3 conductivity on H (see Fig. 6) yields $a = 610$ Å. Consequently, at $\hbar\omega > \varepsilon_3$ photoconductivity takes place over the impurity percolation level. When $\hbar\omega < \varepsilon_3$ (which corresponds to $\lambda = 8$ mm for this sample), we have $a_{ph}^* = 530$ Å, for sample III-7 at all quantum energies we have $a_{ph}^* = 320$ Å, and the photoconductivity is over states near the Fermi level (for III-7 we have $\varepsilon_1 = \varepsilon_F = 20$ meV > 2 meV $= \hbar\omega_{max}$). It is important to note that a_{ph}^* for III-7 is substantially less than for II-3. Indeed, the values of a^* can be estimated from the relation

$$a^* = \hbar / (2me_1)^{1/2}. \quad (11)$$

For sample II-3 calculation in accordance with (11) yields $a^* = 460$ Å, and for III-7 we have $a^* = 150$ Å. For the former sample the values of a^* and a_{ph}^* are close, while for the latter they differ by a factor of two, apparently because (11) does not hold at $\varepsilon_F \gg \varepsilon_d$.

Unfortunately, for the low-compensation sample I-2, whose static conductivity is described by the relation

$$\sigma_s = \sigma_{02} \exp(-\varepsilon_2/kT),$$

it is impossible to carry out a similar analysis, since the influence of H on σ_{02} has not been investigated theoretically. The quantities compared in Fig. 6a are therefore $\mu_{ph}(H)/\mu_{ph}(0)$ and $\sigma_{02}(H)/\sigma_{02}(0)$. The proximity of the curves indicates that photoconductivity over the conducting impurity band⁷ is realized here for all quantum energies. It is important to note that such a "band" photoconductivity goes over in sufficiently strong magnetic fields ($H \geq 7$ kOe) into hopping conductivity and the function $\mu_{ph}(H)$ becomes exponential. At the same values of H , the mechanism of static conductivity also changes: the conductivity over the conducting impurity band gives way to conductivity over the impurity percolation level.

The results of the measurements of $\alpha(H)$ and τ_{ph} confirm the foregoing analysis.

The decrease of α with increasing H for sample II-3 at $\lambda \leq 2$ mm (just as for sample I-2) is due, in our opinion, to the decrease of the cross section for the capture of the photons by the impurity centers. At $\lambda = 8$ mm, owing to the increase in the number of states accessible to the hops of the electrons that produce the photoconductivity, α increases with H , inasmuch as the measurements show that the increase of the binding energy of the hydrogenlike centers is not accompanied by a change in the energy spectrum of the H_2^+ centers, which are the starting levels for the photoelectrons. If the change of the density of the final states is small (sample III-7 at $\lambda \geq 1$ mm), then α takes place only at the highest quantum energies ($\lambda = 0.6$ mm).

The quantity τ_{ph} turns out to be independent of the electric field at all photoconductivity mechanisms, if E is sufficiently weak. A growth of τ_{ph} is observed at values of E where deviation from Ohm's law begins, and is due to the increase of the energy of the hopping photoelectron by an amount eER . At E such that impurity breakdown sets in, τ_{ph} decreases sharply because of the appearance of an appreciable number of free electrons. If μ photoconductivity sets in, τ_{ph} begins to be governed by the relaxation time of the energy of the free electrons.

The latter is apparently small: this is indicated by the predominance of photoconductivity over the impurities, even at $\hbar\omega > \varepsilon_1$. The increase of the concentration of the free electrons explains also the decrease of τ_{ph} at sufficiently large T .

We note also a number of features typical of τ_{ph} in hopping photoconductivity. The maximum of the function $\tau_{ph}(T)$ for photoconductivity over the percolation level indicates apparently that the phonons play a role in the motion of the photoelectrons over the percolation level. The independence of τ_{ph} of the photon energy in hopping photoconductivity over the states near the Fermi level shows that it is determined mainly by the time of electron dissipation of an energy that is low compared with kT .

The aggregate of the results enables us to estimate the volt-watt sensitivity of the samples for the different photoconductivity mechanisms. It turned out, for example, that for sample II-3 in the case of photoconductivity over the percolation level calculation yields $S_u = 10^4$ V/W, as against the measured $S_u \geq 3 \cdot 10^8$ V/W. For photoconductivity over states near the Fermi level, calculation yields $S_u = 2.5 \cdot 10^8$ V/W and measurements $S_u = (1-3) \times 10^8$ V/W.

Thus, the close agreement between the calculated and measured values of the volt-watt sensitivity confirms, in our opinion, the correctness of the proposed model of hopping photoconductivity in n -InSb.

6. CONCLUSION

The results of the investigation of the submillimeter photoconductivity in n -InSb of extremely high purity at helium temperatures show that at any degree of compensation the absorption of the submillimeter radiation is determined mainly by electrons localized on impurities, and the produced photoconductivity is due, independently of the quantum energy, to the motion of the electrons over the impurity states. At $K < 0.8$, the motion of the photoelectrons is over the conducting impurity band; at $K \geq 0.8$ the motion is by hopping. The results of the experiment and of the estimates show that the hopping photoconductivity can be sufficiently high. The hopping photoconductivity is realized not only in n -InSb but also in Ge (Ref. 23) and probably in GaAs (Ref. 36). The hopping photoconductivity mechanism can apparently be substantial for amorphous semiconductors.

¹⁾ The term "hopping photoconductivity" was first introduced by Dobrego and Tyvkin (see, e.g., Ref. 23) to explain the singularities of photoconductivity in n -Ge in interband excitation of the carriers: the photoelectrons are captured by the impurity centers and participate in thermally activated hops over the centers. The magnitude of the effect is determined by the change of the activation energy ε_3 when the concentration of the electrons on the impurities is increased. Bonch-Bruевич and Capek²⁴ have discussed the feasibility, in principle, of photon-stimulated hopping motion of electrons through impurities.

²⁾ An analysis of Anderson's localization criterion¹⁵ shows that in extremely purified n -InSb with $N_d \approx (1-1.5) \times 10^{14} \text{cm}^{-3}$ and

- $K \geq 0.3$ the fluctuation potential¹⁶ is $\gamma \geq 0.5$ Ry and substantially exceeds the overlap integral between the neighboring impurity centers, leading to localization of the impurity states.
- ³ Figure 3 shows plots of $\Delta\sigma(H)$ and not of $\Delta U_{ph}(H)$. This enables us to analyze the influence of H on the photoconductivity, excluding the change of the dark static conductivity with changing H .
- ⁴ The cause of this effect is not yet clear; we shall therefore not consider further the region $H \leq 1$ kOe.
- ⁵ The obtained formula is similar to the formula for the lux-ampere characteristic of an amorphous semiconductor, obtained on the basis of a more rigorous analysis in Ref. 34. It contains, however, a number of unknown parameters, making the estimates difficult.
- ⁶ The formula was obtained for the current-generator regime, and it is assumed that the bias on the sample is maintained constant in the entire temperature range.
- ⁷ We note that in the samples of this group, a certain role can be played by μ photoconductivity, since the concentration of the free electrons at $T = 4.2$ K is $(0.05-0.1) N_g$.²⁶
- ¹ E. H. Putley, Proc. Phys. Soc. London **76**, 802 (1960).
- ² B. V. Rollin, Proc. Phys. Soc. London **77**, 1102 (1961).
- ³ Sh. M. Kogan, Fiz. Tverd. Tela (Leningrad) **4**, 1891 (1962) [Sov. Phys. Solid State **4**, 1386 (1963)].
- ⁴ V. A. Danilychev and B. D. Osipov, Fiz. Tverd. Tela (Leningrad) **5**, 2369 (1963) [Sov. Phys. Solid State **5**, 1724 (1964)].
- ⁵ T. M. Lifshitz, Sh. M. Kogan, A. N. Bystavkin, and P. G. Mel'nik, Zh. Eksp. Teor. Fiz. **42**, 959 (1962) [Sov. Phys. JETP **15**, 661 (1962)].
- ⁶ A. N. Vystavkin, V. N. Gubankov, V. N. Listvin, and V. V. Migulin, Fiz. Tekh. Poluprovodn. **1**, 844 (1967) [Sov. Phys. Semicond. **1**, 702 (1967)].
- ⁷ V. N. Gubankov, Candidate's Dissertation, Institute of Radio and Electronics Sci. USSR, Moscow, 1968.
- ⁸ A. N. Vystavkin and V. V. Migulin, Radiotekh. Elektron. **12**, 1989 (1967).
- ⁹ V. M. Afinogenov and V. I. Trifonov, Fiz. Tekh. Poluprovodn. **6**, 1256 (1972) [Sov. Phys. Semicond. **6**, 1099 (1973)].
- ¹⁰ I. I. Chusov, Fiz. Tekh. Poluprovodn. **8**, 1907 (1974) [Sov. Phys. Semicond. **8**, 1236 (1975)].
- ¹¹ I. I. Chusov and Yu. V. Gulyaev, Fiz. Tekh. Poluprovodn. **8**, 679 (1974) [Sov. Phys. Semicond. **8**, 1040 (1974)].
- ¹² Yu. V. Gulyaev, V. N. Listvin, V. T. Potapov, I. I. Chusov, and N. G. Yaremenko, Fiz. Tekh. Poluprovodn. **9**, 1471 (1975) [Sov. Phys. Semicond. **9**, 972 (1975)].
- ¹³ E. M. Gershenson, V. A. Il'in, L. B. Litvak-Gorskaya, and S. R. Filonovich, Pis'ma Zh. Eksp. Teor. Fiz. **26**, 362 (1977) [JETP Lett. **26**, 243 (1977)].
- ¹⁴ N. F. Mott and E. A. Davis, Electronic Processes in Non-crystalline Materials, Oxford, 1971.
- ¹⁵ P. W. Anderson, Phys. Rev. **109**, 1492 (1958).
- ¹⁶ B. I. Shklovskii and A. L. Efros, Zh. Eksp. Teor. Fiz. **60**, 867 (1970) [Sov. Phys. JETP **33**, 468 (1971)].
- ¹⁷ B. I. Shklovskii, Fiz. Tekh. Poluprovodn. **6**, 1197 (1972) [Sov. Phys. Semicond. **6**, 1053 (1973)].
- ¹⁸ E. M. Gershenson, V. A. Il'in, and L. B. Litvak-Gorskaya, Fiz. Tekh. Poluprovodn. **8**, 295 (1974) [Sov. Phys. Semicond. **8**, 189 (1974)].
- ¹⁹ E. M. Gershenson, V. A. Il'in, I. N. Kurilenko, and L. B. Litvak-Gorskaya, Fiz. Tekh. Poluprovodn. **6**, 1687 (1972) [Sov. Phys. Semicond. **6**, 1457 (1973)].
- ²⁰ V. V. Ardenarchuk, E. M. Gershenson, and L. B. Litvak-Gorskaya, Fiz. Tekh. Poluprovodn. **7**, 132 (1973) [Sov. Phys. Semicond. **7**, 89 (1973)].
- ²¹ V. V. Ardenarchuk, E. M. Gershenson, L. B. Litvak-Gorskaya, and R. I. Rabinovich, Zh. Eksp. Teor. Fiz. **65**, 2387 (1973) [Sov. Phys. JETP **38**, 1192 (1974)].
- ²² N. F. Mott, Philos. Mag. **19**, 835 (1969).
- ²³ V. P. Dobrego and S. M. Tyvkin, Fiz. Tverd. Tela (Leningrad) **6**, 1203 (1964) [Sov. Phys. Solid State **6**, 928 (1964)].
- ²⁴ V. L. Bonch-Bruevich and V. K. Capek, Pis'ma Zh. Eksp. Teor. Fiz. **16**, 109 (1972) [JETP Lett. **16**, 75 (1972)].
- ²⁵ E. M. Gershenson, G. N. Gol'tsman, and N. G. Ptitsina, Zh. Eksp. Teor. Fiz. **64**, 587 (1973) [Sov. Phys. JETP **37**, 299 (1973)].
- ²⁶ V. F. Bannaya, E. M. Gershenson, and L. B. Litvak-Gorskaya, Fiz. Tekh. Poluprovodn. **2**, 978 (1968) [Sov. Phys. Semicond. **2**, 807 (1969)].
- ²⁷ N. I. Fan, transl. in: Usp. Fiz. Nauk **64**, 315 (1958).
- ²⁸ L. A. Orlov, Candidate's Dissertation, Moscow State Pedagogical Institute, 1978.
- ²⁹ E. M. Gershenson, G. N. Gol'tsman, and N. G. Ptitsina, Pis'ma Zh. Eksp. Teor. Fiz. **25**, 574 (1977) [JETP Lett. **25**, 539 (1977)].
- ³⁰ E. M. Gershenson, I. N. Kurilenko, L. B. Litvak-Gorskaya, and R. I. Rabinovich, Fiz. Tekh. Poluprovodn. **7**, 1501 (1973) [Sov. Phys. Semicond. **7**, 1005 (1974)].
- ³¹ E. M. Gershenson, V. S. Ivleva, I. N. Kurilenko, and L. B. Litvak-Gorskaya, Fiz. Tekh. Poluprovodn. **7**, 1982 (1973) [Sov. Phys. Semicond. **7**, 1322 (1974)].
- ³² I. Z. Kostadinov, Pis'ma Zh. Eksp. Teor. Fiz. **14**, 345 (1971); **17**, 44 (1973) [JETP Lett. **14**, 231 (1971)].
- ³³ I. Z. Kostadinov, Proc. of Sixth Internat. Conf. on Amorphous and Liquid Semiconductors, Electronic Phenomena in Non-crystalline Semiconductors, B. T. Kolomiits, ed., Nauka, Leningrad, 1975, p. 156.
- ³⁴ R. Schuhardt and R. Keiper, in Amorphous Semiconductors, **76**, Publ. House of the Hungarian Acad. of Science, Budapest, p. 89.
- ³⁵ T. M. Lifshitz and F. Ya. Nad', Dokl. Acad. Nauk SSSR **162**, 801 (1965) [Sov. Phys. Dokl. **10**, 532 (1965)]; Sh. M. Kogan and B. I. Sedunov, Fiz. Tverd. Tela (Leningrad) **8**, 2382 (1966) [Sov. Phys. Solid State **8**, 1898 (1967)].
- ³⁶ L. V. Berman and A. A. Kal'fa, Fiz. Tekh. Poluprovodn. **10**, 2251 (1976) [Sov. Phys. Semicond. **10**, 1335 (1976)].

Translated by J. G. Adashko